JOURNAL OF PROPULSION AND POWER
Vol. 16, No. 5, September–October 2000

Optimization of Jet Mixing into a Rich, Reacting Crossflow

M. Y. Leong* and G. S. Samuelsen†
University of California, Irvine, Irvine, California 92697-3550
and
J. D. Holdeman‡
NASA John H. Glenn Research Center at Lewis Field, Cleveland, Ohio 44135

Radial jet mixing of pure air into a fuel-rich, reacting crossflow confined to a cylindrical geometry is addressed with a focus on establishing an optimal number of jet orifices. Note that the optimum would not be expected to be universal. That is, the optimum mixer that one would identify will depend on both the momentum–flux ratio and an axial distance appropriate to the application. The number of round holes that most efficiently mixes the jets with the mainstream flow, and thereby minimizes the residence time of near-stoichiometric and unreacted packets, was determined. Such a condition might reduce pollutant formation in axially staged, gas turbine combustor systems. Five different configurations consisting of 8, 10, 12, 14, and 18 round holes are reported. An optimum number of jet orifices is found for a jet to mainstream momentum-flux ratio *J* of 57 and a mass-flow ratio (MR) of 2.5. For this condition, the 14-orifice case produces the lowest spatial unmixedness and the most uniformly distributed species concentration and temperature profiles at a plane located an axial distance equal to one duct diameter from the jet orifice inlet. Note that this is the same configuration that would be identified from non-reacting experiments.

Nomenclature

d = orifice axial length, or round hole diameter
J = jet to mainstream momentum-flux ratio, $(\rho V^2)_{\text{jets}}/(\rho V^2)_{\text{main}}$
MR = jet to mainstream mass-flow ratio, $(\rho VA)_{\text{jets}}/(\rho VA)_{\text{main}}$
n = number of round holes in quick-mix module
R = radius of the quick-mix module
r = radial distance from the module center
T = flowfield temperature
T_{jet} = average temperature of the jets
T_{main} = average mainstream temperature at a plane one duct radius upstream of the jets
U_s = spatial unmixedness
V = velocity
V_{ref} = reference velocity defined at nonreacting inlet conditions
x = axial distance from the leading edge of the orifices
ρ = density
ϕ = equivalence ratio, $(\text{fuel/air})_{\text{local}}/(\text{fuel/air})_{\text{stoichiometric}}$

Introduction

VARIOUS systems, such as fuel injection and exhaust temperature control processes, rely on a rapid and thorough jet mixing with a crossflow of gas to mix streams of fluid. Jet mixing in a crossflow, in fact, may play a fundamental role in the next generation of low-pollutant-emitting engines such as the rich-burn/quick-mix/lean-burn (RQL) combustion concept. The success of this combustor over conventional gas turbine combustors in lowering pollutant production depends on the mixing section between the fuel-rich ($\phi > 1$) and fuel-lean ($\phi < 1$) stages of combustion. In this combustor design, the jets of air introduced through the quick-mixing section mix with the rich reacting crossflow as quickly as possible to bring the reaction to an overall lean equivalence ratio. The formation of various pollutants is driven by high temperatures attained in near-stoichiometric reactions. Therefore, the strategy in this combustor design lies in minimizing the lifetime of, as well as preventing the formation of, near-stoichiometric fluid packets. As passing through stoichiometric regions is inevitable, rapid mixing reduces the lifetime of the stoichiometric packets, and the production of a uniform fuel-lean mixture precludes their formation.

A previous study by the authors[1] involved the construction of a facility that handled reacting tests in a cylindrical crossflow configuration. A particular jet orifice geometry, the 10 round hole case, was tested to explore the types of information that could be gathered from the experiment. The current study expands on this initial work by addressing whether, for a given jet to crossflow momentum-flux ratio and mass-flow ratio (MR), a configuration with an optimal number of orifices can yield rapid mixing of pure air jets into a rich crossflow and result in a uniformly lean mixture with minimal potential for pollutant formation.

Background

The gas turbine combustor exhibits many examples of jet mixing in a reacting crossflow, as evidenced by the presence of air ports in the primary, intermediate, and dilution zones of conventional combustors. An understanding of the jet-mixing process becomes important in guiding the design of the ports to obtain the desired mixing fields for given operating conditions. The prediction of jet mixing in combusting flows is especially important in an application such as the quick-mix section of the RQL combustor, where poor mixing of the jets of air with the rich, reacting crossflow leads to hot pockets conducive to pollutant formation. The nonreacting, multiple jet-in-crossflow experiment is a tool to address this problem, because it is an inexpensive and convenient method for predicting mixing fields in combusting flows.

Numerous studies on the nonreacting jet-in-crossflow problem have investigated the resultant mixing phenomena of vortex development and crossflow fluid entrainment, both of which determine the structure and penetration of the jet. An extensive listing of these documented jet-in-crossflow studies performed in the past few decades can be found in Refs. 2–5. Note that many of the studies cited in these summaries are of a single jet in an unbounded crossflow or are otherwise inappropriate for direct application. Although the single jet is a key component in combustor flowfields, these flows are usually confined, and interaction between jets is critical. Also, because the references listed in Refs. 2–5 are extensive, only those papers from which specific material is mentioned will be cited in this paper.

Received 30 June 1998; revision received 20 June 1999; accepted for publication 8 July 1999.

*Graduate Researcher, University of California at Irvine Combustion Laboratory. Student Member AIAA.
†Professor, University of California at Irvine Combustion Laboratory; gss@uci.edu. Associate Fellow AIAA.
‡Senior Research Engineer, Turbomachinery and Propulsion Systems Division. Associate Fellow AIAA.

Although the jet-mixing studies illustrate much activity with respect to a nonreacting system, research into reacting jet-in-crossflow systems has been limited. Tests on multiple jet mixing in reacting flows have mainly been performed on model gas turbine combustors of a can type, or cylindrical duct geometry. In many of these experiments,[6–9] the model gas turbine combustors contained two sets of holes for primary and dilution air mixing that are typically found in conventional combustors, as opposed to the single-stage, quick-mixing scheme that is present in an RQL configuration. These studies were also concerned with varying operating conditions such as fuel injection,[6] air preheat,[7] fuel–air ratio,[8] or the momentum–flux ratio of the primary jets.[9] In one study, a geometric parameterization was pursued, but with the main objective of varying the positions of the rows of the primary and dilution jets rather than with changing the orifice configurations.[9]

Outside of the conventional combustor experiments, few reacting RQL combustor studies have been conducted. In one study, NO_x emissions were measured from a model RQL combustor operating at various pressures and inlet temperatures, but only for a 20 round hole quick-mixing section.[10] However, the results from this RQL study did emphasize that the optimization of the quick-mixing section was integral in lowering the total NO_x emissions from the RQL combustor.

In general, these conventional and RQL combustor tests varied operating parameters to affect the distributions of emissions and temperature. The current study, on the other hand, affects jet mixing with the reacting crossflow by varying the number of orifices at a set momentum–flux ratio. Multiple jet mixing with a reacting crossflow confined to a cylindrical duct was the subject of a recent study in which tests were conducted at a momentum–flux ratio targeting the RQL operating condition.[1] The present study applies the diagnostic tools and analysis utilized in Ref. 1 to build on a series of related work performed on a nonreacting, multiple jet mixing in a cylindrical duct system. The nonreacting studies, which include Refs. 11 and 12, surveyed the effect of the jet to crossflow momentum–flux ratio and the shape, orientation, and number of orifices on jet penetration and mixing. Optimal orifice configurations were designated as those that produced uniform mixing within a specified length, for example, one duct radius from jet injection. With dependence on the chosen jet to crossflow momentum–flux ratio J and the orifice spacing to duct height ratio S/H, various optimal orifice configurations were obtained. However, it was unknown if an optimum configuration identified through nonreacting experiments would apply in reacting flows.

The objectives for this study are to determine an effect between jet mixing and the achievement of desired outlet conditions and to identify an orifice configuration leading to optimal mixing at a specific jet to crossflow momentum–flux ratio and a specific MR. For the reacting experiment, optimal mixing is attained when the desired outlet conditions of reaction completeness and lower temperatures associated with a uniformly lean mixture are satisfied.

Experiment

The facility utilized for the current reacting jet-in-crossflow mixing tests was previously used in the study described in Ref. 1. Although a general description of the test facility as well as the measurement protocol are detailed in this section, additional details and specifications can be found in Refs. 1 and 13.

Facility

The facility consisted of a rich product generator and a jet-mixing section (Fig. 1). The rich product generator mixed propane gas with air upstream of the ignition point. Combustion occurred in a zone stabilized by a swirler. To dissipate the swirl in the flow and to introduce a uniform nonswirling flow into the jet-mixing section, the rich product was passed through an oxide-bonded silicon carbide (OBSiC) ceramic foam matrix produced by Hi-Tech Ceramics with a rated porosity of 4 pores/cm (10 pores/in.).

The mixing section comprises a modular quartz section to which the jets of air were supplied from the surrounding plenum. The plenum was fed by four equally spaced, individually metered air ports located toward the base of the plenum. A high-temperature steel flow straightener installed in the plenum conditioned and equally distributed the jets of air entering the mixing module.

Table 1 Orifice geometry specifications for each quick-mix module

Number of orifices, n	Orifice diameter d, mm	Blockage, $nd/(2\pi R)$
8	14.0	0.447
10	12.5	0.499
12	11.5	0.547
14	10.6	0.591
18	9.4	0.670

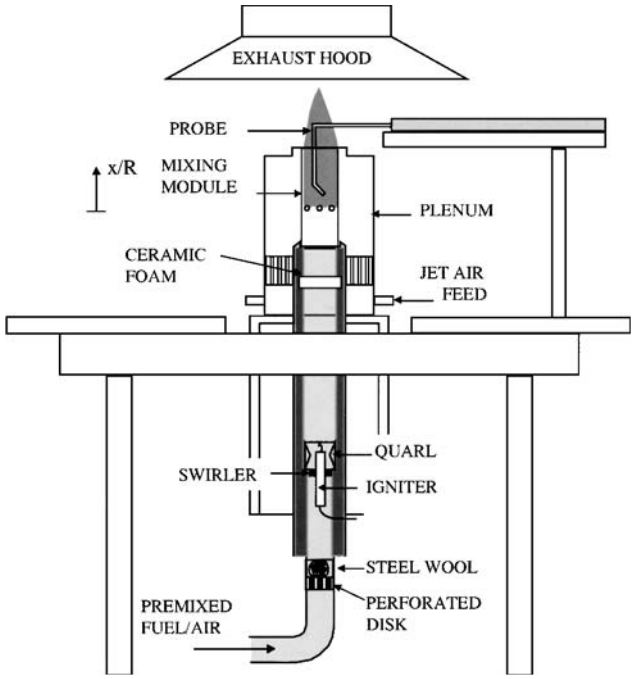

Fig. 1 Reacting flow test stand.

An alumina–silica blend of ceramic fiber paper provided sealing between the quartz module and the stainless steel mating surfaces. The modules tested were the 8-, 10-, 12-, 14-, and 18-orifice configurations. The 10 round hole module results were previously discussed in Ref. 1.

The quartz modules were 280 mm (11 in.) in length, with inner and outer wall diameters of 80 mm (3.15 in.) and 85 mm (3.35 in.). The row of orifices was positioned with its centerline 115 mm (4.5 in.) downstream from the module entrance. Table 1 lists for each configuration the orifice diameter and blockage, which is a ratio that compares the projection of the orifice onto the module circumference to the circumferential spacing between orifice centers.

The experiments were performed at a jet to mainstream momentum–flux ratio J of 57. J is the ratio of the total momentum flux for all jets entering the module to the momentum flux of the crossflow defined by its properties at plane 1 in the rich section (see Fig. 2) and is equivalent to the J for an individual jet (note that J is a flux ratio, and so it does not include the orifice area). The ratio of the mass-flow rates (MR) of the overall jet flow to the crossflow was 2.5 in this experiment. MR and J were kept constant by maintaining the same overall jet orifice area for each module. The total effective area of the orifices was 903 mm^2 (1.40 $in.^2$) for each mixing module, which resulted in the diameters of the orifices changing for each orifice number configuration (see Table 1). The ratio of the total effective jet area to the duct cross-sectional area was 0.18, and the ratio of the total geometric jet area to the duct cross-sectional area was 0.27. The fuel, mainstream air, and jet airflow rates were determined by the MR as well as by the ϕ of the rich and lean sections. The operating conditions are noted in Table 2.

Table 2 Operating conditions

Parameter	Value
Ambient pressure, atm	1
Rich equivalence ratio ϕ	1.66
Overall equivalence ratio ϕ	0.45
Mainstream temperature T_{main}, K	1500
Jet temperature T_{jet}, K	480
Reference velocity V_{ref}, m/s	18
Fuel mass-flow rate, kg/s	0.00296
Mainstream air mass-flow rate, kg/s	0.0275
Jet air mass-flow rate, kg/s	0.0752
Jet to mainstream momentum-flux ratio J	57
Overall jet to crossflow MR	2.5
Overall jet to crossflow density ratio	3.3

Table 3 Location of planes with respect to leading edge of orifices

Plane	Position	x/R
1	One module radius upstream	-1
2	Orifice leading edge	0
3	One-half of the orifice length	$(d/2)/R$
4	Orifice length (trailing edge)	d/R
5	One module radius downstream	1
6	Two module radii downstream	2

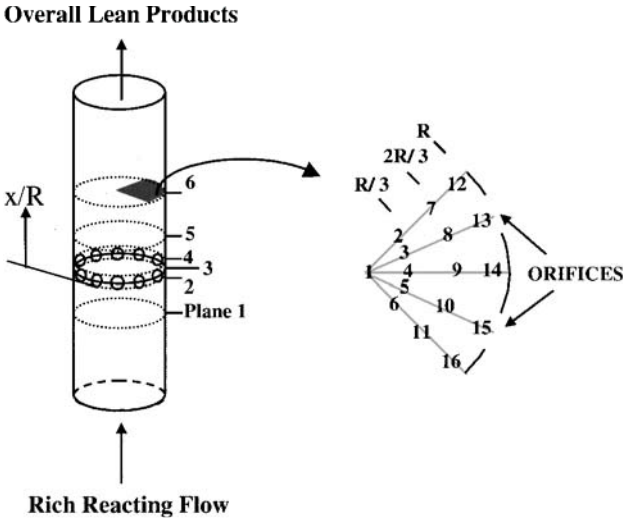

Fig. 2 Measurement locations.

Measurement Protocols

Temperature and species concentration data were obtained in a sector grid for six planes (Fig. 2) for each module. With respect to the leading edge of the orifices, the planes were located in the positions shown in Table 3.

Each planar grid consisted of 16 points arranged over a region that included two orifices (see Fig. 2). One point was positioned at the center, and five points were placed along each of the arc lengths of $r/R = \frac{1}{3}$, $\frac{2}{3}$, and 1. The points along each arc were distributed such that two radii of points were aligned with the center of the orifices and three radii were aligned with the midpoint between orifice centers.

A water-cooled probe with an outer diameter of 7.95 mm (0.313 in.) was utilized in the temperature and species concentration measurements. For temperature measurements, a type B thermocouple comprising a pair of bare platinum–rhodium wires 0.254 mm (0.010 in.) in diameter was threaded through the sample extraction tube and positioned such that the junction extended 2.54 mm (0.10 in.) beyond the probe tip. The thermocouple junction, created by spot welding the wires, resulted in a mean bead diameter of 0.381 mm (0.015 in.). A computer program recorded and returned an average of 100 readings after a span of 20 s. The calculated frequency response of the thermocouple was greater than 5 Hz, which was verified in the recorded data. Instrument uncertainty resulted in a maximum variation in temperature measurement of 2.5%.

Species concentration measurements were obtained by routing the sample through a heated line connected to the emission analyzers. Water was condensed from the gas before the sample was analyzed by nondispersed infrared, paramagnetic, and flame ionization detection. A data acquisition program read 100 samples in 20 s and returned an averaged quantity. The uncertainty in the measurement of the species concentration was 1% of the full-scale reading of the analyzer range.

Analyses

The jet mixture fraction was derived from conserved scalar calculations of the mass fraction of carbon. To obtain the carbon mass fraction at each datum point, the dry species concentration measurements were first converted to wet mole fractions. The wet mole fractions were calculated by solving a system of eight linear equations that included the measured dry species concentrations of CO, CO_2, O_2, and unburned HC (assumed to be composed mainly of unburned C_3H_8), as well as C_2H_4, H_2, N_2, and H_2O (Ref. 14). The inclusion of C_2H_4, which is a prevalent intermediate species produced from the combustion of C_3H_8 (Ref. 15), was necessary to form a closed set of equations. The calculated unburned hydrocarbon species C_3H_8 and C_2H_4 contributed, at most, to 1.4% of the overall wet mole fraction at each point. The concentration of H_2, a primary species of combustion produced under fuel-rich reactions, was assumed to be 65% of the concentration of CO (Ref. 14). N_2 was assumed to make up the rest of the gas concentration in the sample.

Once the wet mole fractions of the species were calculated, the carbon mass fraction Y was obtained and substituted into the relationship for the jet mixture fraction f calculated at each point for this system,

$$f = 1 - \frac{Y_{\text{sample}}}{Y_{\text{main}}} \tag{1}$$

where Y_{sample} refers to the carbon mass fraction derived from the measured species concentrations and Y_{main} refers to the carbon mass fraction calculated from the metered fuel and air mass-flow rates in the rich section.

To determine the round hole configuration leading to the most uniform mixture of chemical species at the different planes, a parameter called spatial unmixedness U_s was used. U_s is a normalized variance that quantifies planar mixing[16] and is a modified version of the definition of temporal unmixedness U obtained at a point.[17] The use of time-averaged values across a spatial domain to calculate planar unmixedness was validated in Ref. 18, where a comparison between the value of U computed from an ensemble of instantaneous concentrations across the plane, and the value of U_s calculated from time-averaged concentrations per point, showed both values being nearly identical. The spatial unmixedness can, thus, be defined as

$$U_s = f_{\text{var}}/f_{\text{av}}(1 - f_{\text{av}}) \tag{2}$$

where f_{var} refers to the variance of all f in a plane that deviates from f_{av}, the area-weighted average jet mixture fraction specific to each plane. The advantage of utilizing U_s to quantify and compare planar mixing between different cases lies in the bounded nature of the parameter. U_s values are bounded between 0 and 1, with the former corresponding to perfect fuel–air mixing and the latter referring to the complete segregation of fuel and air in the plane.

Results and Discussion

Temperature and species concentrations measured at the rich inlet crossflow (plane 1) showed near-uniform distributions for each module tested. The temporal fluctuations derived from the recorded temperatures revealed a maximum fluctuation of 0.4% across all of the measured points in plane 1. The average temperature was 1500 K with a 1% uncertainty, and the average concentrations of O_2, CO, and CO_2 across all of the modules were 0, 12.5, and 5.25%,

respectively, with an uncertainty of 0.1%. For all of the module configurations tested, the maximum U_s value at plane 1 was 0.0064, which suggests a near-homogeneous spatial composition. Because of the uniformity in the measured data, distributions at plane 1 are not included in the contour plots that show the spatial distribution of the flowfield measurements.

Jet Penetration and Reaction

Temperature Profiles

In combustor design, the attainment of a short combustor length is desired to maintain the compactness of the engine. Because the RQL configuration is an axially staged device, it is preferable to attain complete mixing and reaction within a minimal length. Nonreacting studies performed in Refs. 11 and 12 utilized an axial distance corresponding to one duct radius as an arbitrary reference plane of comparison. However, in initial reacting tests performed on the system,[1] it was shown that the reaction continues beyond this mixing length. Therefore, for the basis of this comparison between the five mixing modules, optimal mixing and reaction is determined within one duct diameter (or two duct radii) of the jet entrance, that is, at plane 6.

Figure 3 shows the evolution of temperature-related profiles for all of the cases tested. The temperatures are normalized with respect to the area-weighted average obtained at plane 1 in the rich zone T_{main}. For a nonreacting flowfield with the same mainstream and jet inlet temperatures of 1500 and 480 K, respectively, a fully mixed system would result in a normalized equilibrium temperature of $T_{\text{equil}}/T_{\text{main}} = 0.514$. As seen from the values in the planes downstream of the orifices, the distributions are well above this value for all of the cases and, thus, indicate both the presence of reaction and the fact that temperature is not a conserved scalar in a reacting flow.

In each of the cases tested, cooler wall temperatures exist at the orifice leading edge at plane 2. Heat loss occurs near the wall region as heat is transferred from the mixing module out through the wall, which is cooled by the air in the jet plenum feed. The jet fluid is denoted by values ranging between 0.263 and 0.306 and is shown entering the module at plane 3. The presence of the jets is also denoted by increased temporal fluctuations of up to 5% at points that are in line with the jets, for example, points 13 and 15. By plane 4, all of the jet fluid has entered the crossflow and has started to disperse across the entire sector. The jet fluid dispersion corresponds to increased temporal fluctuations of up to 10% in the jet injection region (points 8, 10, 13, and 15). As the number of holes increases, jet penetration also decreases and allows more of the reacting crossflow to pass through the center of the module.

Between the orifice region and the one-radius distance (plane 5), most of the mixing has occurred. The maximum fluctuations in temperature decrease to 5% at plane 5 and to 4% at plane 6. The resultant mixing and reaction between the jet fluid and the rich crossflow leads to a stratification of temperature for all of the modules. At planes downstream of the orifices, the position and magnitude of the lower temperature bands vary with respect to the number of orifices. By Plane 6, the eight-orifice case shows values of T/T_{main} between 0.540 and 0.622 occurring in the core of the duct that is defined by the location of points 1–6. The 10- and 12-orifice cases also produce a flowfield with lower temperatures occurring toward the center of the module at plane 6, but with lows of T/T_{main} varying from 0.659 to 0.752 in the 10-orifice case and T/T_{main} varying from 0.759 to 0.952 in the 12-orifice case. In all of these cases, the 8-, 10-, and 12-orifice modules show a band of T/T_{main}, 110% and greater, occurring along the wall region.

In the case of the 14- and 18-orifice modules, both yield lower temperature bands near the half-radius of the mixing section at plane 5 (in the 0.70–0.80 range). Subsequent mixing and reaction lead to the low T/T_{main} bands of green occurring near the half-radius for both the 14- and 18-orifice modules. Though the 18-orifice case achieves lower T/T_{main} values than does the 14-orifice case, the temperature distributions are more uniform across plane 6 for the 14-orifice case.

In a cylindrical duct, the half-area radius of the mixer is defined as the radius that divides the duct cross section into equal cylindrical and annular areas. Whereas the half-area radius has a value of $r = R/(2)^{1/2}$, the half-radius of the cylindrical duct is represented by $r = R/2$. Using these definitions, a jet whose trajectory falls between the injection wall and the half-area radius is termed underpenetrating, a jet whose trajectory falls between the half-area radius and half-radius is labeled optimal in penetration, whereas a jet whose trajectory falls between the half-radius and the center of the duct is called overpenetrating. Thus, the eight-orifice case produces jet overpenetration that results in a hot wall region and a cooler core region. The 10- and 12-orifice cases show results that are similar, but not as extreme as the 8-orifice case, and are considered slightly overpenetrating. The 18-orifice case, on the other hand, produces a reversed stratified distribution with a hotter core region and a cooler wall region characteristic of jet underpenetration. Finally,

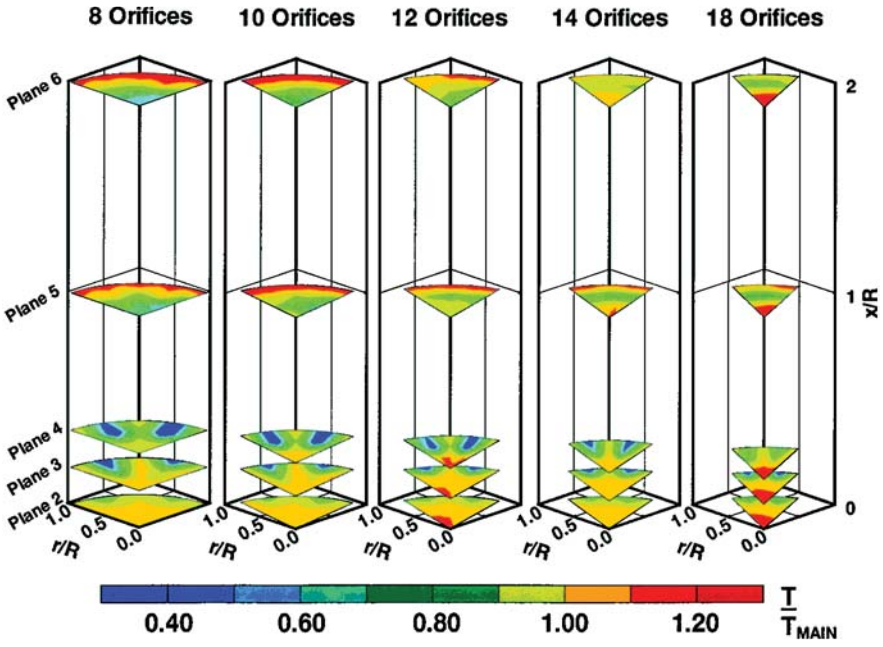

Fig. 3 Temperature profile comparison.

the 14-orifice case is considered optimal because the penetration of the jets lies between the half-area radius and half-radius, which leads to a more uniform distribution of temperature.

In addition to the temperature distributions, the centerline temperatures in Fig. 4 also corroborate the designation of the over-, under-, and optimally penetrating cases. The temperature ratios shown at plane 6, with a T/T_{main} uncertainty of ± 0.03, reflect significantly different values. For all of the modules, the centerline temperature remains nearly constant in the regions upstream of and within the orifice planes. Jet penetration to the centerline is indicated by a dip in the temperature relative to the initial rich reacting temperature. Jet overpenetration, denoted by the persisting presence of cooler jet fluid at plane 5, can, therefore, be found in the 8-, 10-, and 12-orifice cases. The 14- and 18-orifice cases show centerline temperatures that are at or above their initial plane 1 values and suggest either optimally penetrating or underpenetrating jets. The number of round holes affects the degree of penetration: as the number of orifices increases from 8 to 18, jet penetration transitions from over- to underpenetration.

Species Concentration Profiles

The effect of the number of orifices on jet penetration is also illustrated in the O_2 distributions of Fig. 5. The jet trajectory is defined by the locus of points showing maximal O_2 concentration as a function of distance because the mainstream contains no oxygen.

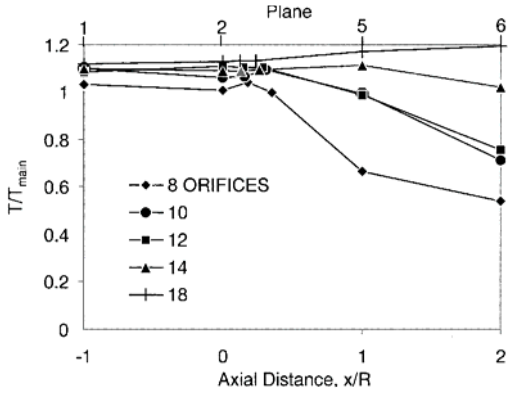

Fig. 4 Centerline temperature history.

At plane 4, a larger bulk of jet fluid enters through each orifice in the 8 round hole case, and a successive decrease in jet fluid per orifice occurs as the number of orifices increases. This decrease in mass flow per orifice is related to the decrease in the individual jet orifice area because the jet velocity through each orifice is constant for all five configurations. As the number of orifices increases, jet penetration into the crossflow diminishes because the jet spacing decreases. Jet spacing affects the interaction between adjacent jets and affects the blockage of the crossflow by the jets, which in turn can affect jet penetration by directing the crossflow toward the center of the duct. Note that an increase in the number of orifices leads to an increase in blockage (see Table 1).

At plane 5, overpenetration causes the jet fluid to impinge at the centerline in the 8-orifice case and results in a high concentration of O_2 in the central core (between 16.8 and 18.4% at plane 6). Overpenetrating jets are undesirable because the oxygen accumulates in the center and reduces the mixing and reaction of the jets of air with the crossflow. The 10- and 12-orifice cases also exhibit overpenetration as the jet trajectory intersects with the centerline at plane 6. In the central core region at plane 6, the measured O_2 concentrations varied between 13.9 and 16.7% for the 10-orifice case, and between 12.9 and 14.8% for the 12-orifice case. At the same plane, the overall O_2 levels for the 14- and 18-orifice cases were no higher than 13%.

As with jet overpenetration, jet underpenetration decreases the extent of mixing and reaction because the jet fluid is bounded in part by the wall of the module. Jet underpenetration, as shown by the high O_2 concentration band between the half-area radius and the wall in the 18-orifice case, allows the rich reaction products to exit the module through the core of the duct without completing the combustion process, which is undesirable. In the more optimally-penetrating 14-orifice case, the jets are exposed to the crossflow along both inner and outer surfaces, which accelerates O_2 dispersion such that the rich mainstream flow reacts with rather than bypasses the jets of air.

The experiment was designed to transition from a $\phi = 1.66$, fuel-rich section to a $\phi = 0.45$, fuel-lean section. The equivalence ratio profiles in Fig. 6 help to determine the extent that the flow achieves a uniformly lean design condition. The crossflow entering the jet mixing zone at plane 2 consists of a uniform rich flow with $\phi = 1.60$. By plane 5, the equivalence ratios are distributed in stratified ranges. At this plane, the 8-, 10-, and 12-orifice cases show near-stoichiometric contours in the wake of the jets whereas the 14- and 18-orifice cases show rich effluent near the centerline. By plane 6, the flowfields show that an overall lean equivalence ratio is attained for all

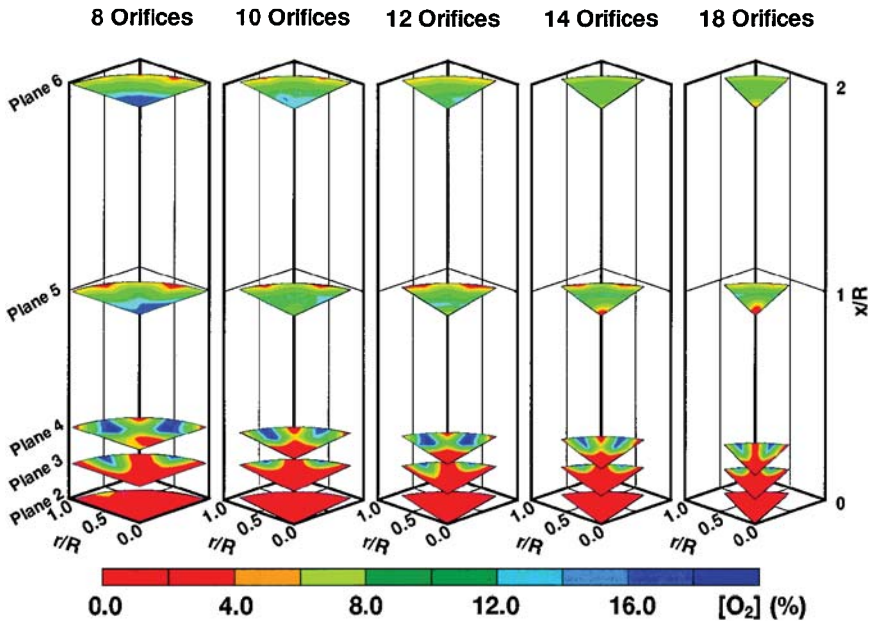

Fig. 5 O_2 concentration profiles.

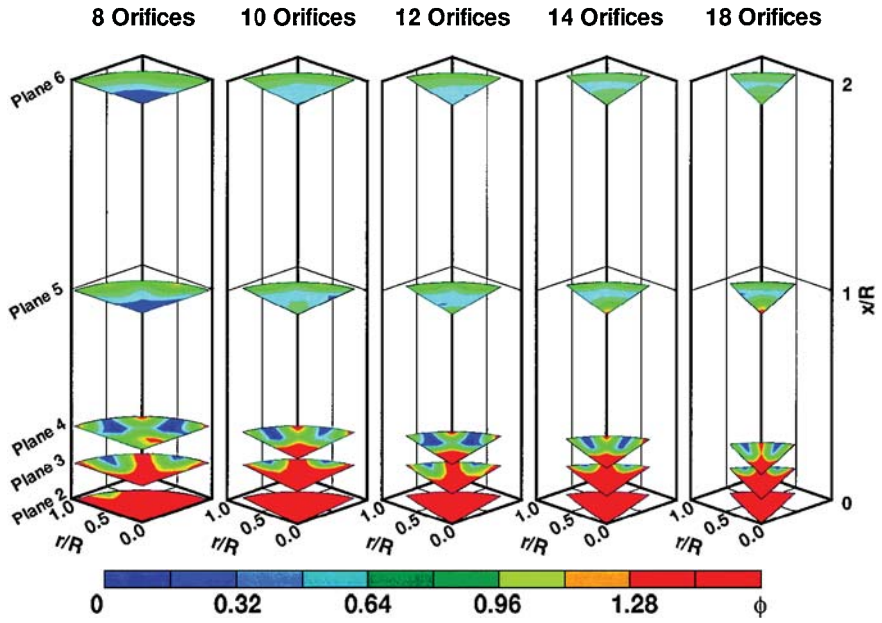

Fig. 6 Equivalence ratio profiles.

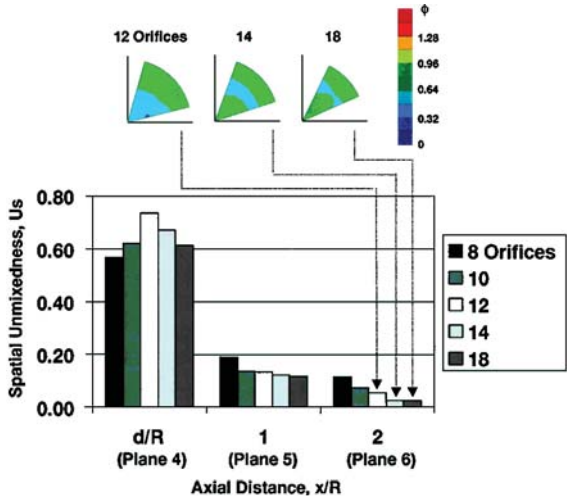

Fig. 7 Comparison of spatial unmixedness values calculated per plane.

cases, though with varying degrees of mixedness. For example, near-stoichiometric equivalence ratios between 0.9 and 1.0 occur along the wall for the 8- and 10-orifice cases and at the centerline for the 18-orifice case. The 12-orifice case produces high equivalence ratios near 0.8 along the wall. The 14-orifice case, on the other hand, shows a relatively more uniform distribution of ϕ, which signifies good mixing.

Spatial Unmixedness

Figure 7 compares the planar spatial unmixedness values derived from the jet mixture fractions at each plane. The spatial unmixedness in the flowfield is assessed and compared at plane 4 and beyond, after all of the jet fluid has entered the crossflow. At plane 4, U_s ranges from a low of 0.57 for the 8-orifice case to a high of 0.73 for the 12-orifice case. The subsequent mixing of the jets with the crossflow reduces U_s to levels under 0.20. At plane 5, the 8-orifice module exhibits a U_s of 0.19 that is relatively higher than the values for the rest of the modules. As the number of orifices increases from 12 to 18, U_s decreases from 0.14 to 0.12. The large difference between the U_s values at planes 4 and 5 may be related to that the mixing is more turbulent at plane 4 (near the orifices) than at plane 5 (downstream of the orifices).

The U_s values at plane 6 also show an overall reduction from the values in plane 5. However, the trend in the relationship between U_s and the number of orifices, as seen in plane 5, recurs in plane 6. The 8-orifice module, with $U_s = 0.11$, continues to show a higher spatial unmixedness than do the other cases. U_s decreases as the number of orifices increases up until the 14-orifice case. For this configuration, $U_s = 0.026$, which is identical to the U_s value for the 18-orifice case.

The spatial unmixedness indicates the extent of mixing occurring between the rich crossflow and the air, but not the degree of reaction between the two streams. From the temperature profiles in Fig. 3 and the equivalence ratio profiles in Fig. 6, the most desired combination of lower overall temperatures and leaner equivalence ratio fields occurs somewhere between the 12 and the 14 round hole cases (see also the enlarged equivalence ratio plots in Fig. 7). The 18-orifice case also produces as low a spatial unmixedness as the 14-orifice case, but the underpenetrating jets in the 18-orifice case produce a hot core of near-stoichiometric reacting fluid that persists in the lean reaction region. Hence, of the 14 and 18 round hole cases, the 14-orifice case produces the optimal case of good overall mixing and reaction. Note that both the U_s and the measured distributions need to be considered in identifying an optimal configuration.[3–5] Other reasons for choosing the 14-orifice case over the 18-orifice module can be made from a practical standpoint. Because fewer holes need to be drilled, the 14-orifice case is easier to manufacture. With fewer holes, more material is also left between the orifices, which helps in maintaining the structural integrity of the mixing section.

Optimum Number of Round Holes

For cylindrical crossflow geometries, several investigations have determined a jet penetration depth that leads to better mixing. Results from a numerical study in Ref. 19 suggest that optimal mixing occurs when the jet penetrates to the half-radius. Reference 12 infers from non-reacting experimental results that optimal mixing occurs when the jet penetrates to the half-area radius (at a radial distance 30% from the wall). For the cases tested in the current study, the jet trajectory from the wall (indicated by both temperature and O_2 profiles) intersects plane 5, 1) beyond the half-radius in the 8- and 10-orifice cases, 2) just beyond the half-radius in the 12-orifice case, and 3) at a point between the half-radius and half-area radius in the 14- and 18-orifice cases. The criterion from Ref. 19 supports the 12- or 14-orifice cases as candidates leading to jet penetration that promotes the best mixing, whereas Ref. 12 supports either the 14- or 18-orifice case as the optimal configuration.

For multiple jet injection into a nonreacting crossflow, Holdeman[3] notes that optimal jet penetration and mixing is determined by J and the orifice spacing to duct height ratio S/H. The following relationship,

$$C = (S/H)\sqrt{J} \tag{3}$$

in which C is an empirical constant that depends on the injection scheme, shows that the two parameters are inversely related. Assuming that the orifice spacing and momentum-flux ratio for a rectangular duct occurs at the radius that divides the can into equal-area cylindrical and annular sections (the half-area radius), the relationship for cylindrically confined crossflows as derived from Eq. (3) is

$$n = \pi\sqrt{2J}/C \tag{4}$$

where $C = 2.5$ for optimal mixing of a single row of round holes.[3] Note that in Eq. (4), the S/H ratio is represented by the number of orifices n.

In the reacting experiment where $J = 57$, Eq. (4) yields an optimal configuration of 13 orifices, which is the whole number rounded up from $n = 12.8$. This calculation corroborates the designation of the 14-orifice case as the optimal reacting case tested, but also suggests that distributions of an even higher, if not comparable, uniformity may be attained for a 13-orifice configuration.

Conclusions

An experiment was performed to provide a test bed for the study of jet mixing in a uniform, nonswirling, rich reacting environment. In this demonstration, it was possible to relate the jet penetration with reacting and mixing fields for five round hole configurations.

For a momentum–flux ratio $J = 57$ and MR $= 2.5$ (under atmospheric pressure) the following was found:

1) When jet penetration increases beyond optimal as in the 8-orifice case, the jet mass accumulates in the central core of the mixer rather than dispersing radially throughout the quick-mix module. Unmixed and unreacted rich crossflow product flows through the jet mixing region along the circumference of the wall.

2) Conversely, when jet penetration decreases below the optimal point such as in the 18-orifice case, a hotter core of fluid bypasses the jet region without completing the reaction toward the desired fuel-lean state.

3) The bulk of jet reaction and mixing occurs before the $x/R = 1$ plane (plane 5).

4) Considering both mixing and completeness of reaction, the 14-orifice module, which exhibits jet penetration between the mixer half-radius and half-area radius at the $x/R = 1$ plane (plane 5), appears to be the best configuration tested. Thorough mixing, as represented by a low spatial unmixedness and completeness of reaction, leads to the attainment of a uniform mixture of complete combustion products at the desired lean equivalence ratio. A goal of the mixing section is to achieve low spatial unmixedness values as close to the orifice region as possible, although, as pointed out in Refs. 4 and 5, one must also peruse the corresponding distributions to avoid identifying an inappropriate choice as best.

Acknowledgment

This work was supported by a Grant from the NASA John H. Glenn Research Center at Lewis Field (Grant NAG3-1110).

References

[1] Leong, M. Y., Samuelsen, G. S., and Holdeman, J. D., "Mixing of Air Jets with a Fuel-Rich, Reacting Crossflow," *Journal of Propulsion and Power*, Vol. 15, No. 2, 1999, pp. 1–6; also NASA TM-107430, 1997.

[2] Margason, R. J., "Fifty Years of Jet in Cross Flow Research," *Computational and Experimental Assessment of Jets in Cross Flow*, CP-534, AGARD 1993.

[3] Holdeman, J. D., "Mixing of Multiple Jets with a Confined Subsonic Crossflow," *Progress in Energy and Combustion Science*, Vol. 19, No. 1, 1993, pp. 31–70; also NASA TM-104412, 1991.

[4] Holdeman, J. D., Liscinsky, D. S., Oechsle, V. L., Samuelsen, G. S., and Smith, C. E., "Mixing of Multiple Jets with a Confined Subsonic Crossflow: Part I—Cylindrical Duct," *Journal of Engineering for Gas Turbines and Power*, Vol. 119, No. 4, 1997, pp. 852–862; also American Society of Mechanical Engineers Paper 96-GT-482, June 1996 and NASA TM-107185, 1996.

[5] Holdeman, J. D., Liscinsky, D. S., and Bain, D. B., "Mixing of Multiple Jets with a Confined Subsonic Crossflow: Part II—Opposed Rows of Orifices in a Rectangular Duct," *Journal of Engineering for Gas Turbines and Power* Vol. 121, 1999, pp. 551–562; also NASA TM-107461, 1996.

[6] Noyce, J. R., Sheppard, C. G. W., and Yamba, F. D., "Measurements of Mixing and Species Concentration Within a Gas Turbine Type Combustor," *Combustion Science and Technology*, Vol. 25, Nos. 5 and 6, 1981, pp. 209–217.

[7] Bicen, A. F., Tse, D. G. N., and Whitelaw, J. H., "Combustion Characteristics of a Model Can-Type Combustor," *Combustion and Flame*, Vol. 80, No. 2, 1990, pp. 111–125.

[8] Heitor, M. V., and Whitelaw, J. H., "Velocity, Temperature, and Species Characteristics of the Flow in a Gas-Turbine Combustor," *Combustion and Flame*, Vol. 64, No. 1, 1986, pp. 1–32.

[9] Richards, C. D., and Samuelsen, G. S., "The Role of Primary Jet Injection on Mixing in Gas Turbine Combustion," *Proceedings of the Twenty-Third International Symposium on Combustion*, Vol. 23, Combustion Inst., Pittsburgh, PA, 1990, pp. 1071–1077.

[10] Meisl, J., Koch, R., Kneer, R., and Wittig, S., "Study of NO_x Emission Characteristics in Pressurized Staged Combustor Concepts," *Proceedings of the Twenty-Fifth International Symposium on Combustion*, Vol. 25, Combustion Inst., Pittsburgh, PA, 1994, pp. 1043–1049.

[11] Hatch, M. S., Sowa, W. A., Samuelsen, G. S., and Holdeman, J. D., "Jet Mixing into a Heated Cross Flow in a Cylindrical Duct: Influence of Geometry and Flow Variations," *Journal of Propulsion and Power*, Vol. 11, No. 3, 1995, pp. 393–402; also NASA TM-105390, 1992.

[12] Kroll, J. T., Sowa, W. A., Samuelsen, G. S., and Holdeman, J. D., "Optimization of Circular Orifice Jets Mixing into a Heated Cross Flow in a Cylindrical Duct," AIAA Paper 93-0249, Jan. 1993; also NASA TM-105984, 1993.

[13] Leong, M. Y., and Samuelsen, G. S., "Quick-Mixing Studies Under Reacting Conditions," NASA CR 195375, Sept. 1996.

[14] Jones, W. P., McDonell, V., McGuirk, J. J., Milosavljevic, V. D., Taylor, A. M. K. P., and Whitelaw, J. H., "The Calculation of Mean Mixture Fractions in Turbulent Non-Premixed Methane Flames from Aspiration-Probe Measurements," Rept. TF/93/13, Dept. of Mechanical Engineering, Imperial College of Science, Technology, and Medicine, London, England, U.K., 1993.

[15] Glassman, I., *Combustion*, Academic, Orlando, FL, 1987, p. 89.

[16] Liscinsky, D. S., True, B., and Holdeman, J. D., "Experimental Investigation of Crossflow Jet Mixing in a Rectangular Duct," AIAA Paper 93-2037, July 1993; also NASA TM-106152, 1993.

[17] Danckwertz, P. V., "The Definition and Measurement of Some Characteristics of Mixtures," *Applied Scientific Research*, Sec. A, Vol. 3, No. 4, 1952, pp. 279–296.

[18] Vranos, A., Liscinsky, D. S., True, B., and Holdeman, J. D., "Experimental Study of Cross-Stream Mixing in a Cylindrical Duct," AIAA Paper 91-2459, June 1991; also NASA TM-105180, 1991.

[19] Talpallikar, M. V., Smith, C. E., Lai, M. C., and Holdeman, J. D., "CFD Analysis of Jet Mixing in Low NO_x Flametube Combustors," *Journal of Engineering for Gas Turbines and Power*, Vol. 114, No. 2, 1992, pp. 416–424; also NASA TM-104466, 1991.